Bulgarian Journal of Physics vol. **51** (2024) 296–310

Geodesic Characteristics of the Black Hole in Bardeen AdS with Quintessence and Super-Radiant Effect

Indrajit Halder [1,2], **Kamal Lochan Mahanta** [2*], **Rakesh Ranjan Sahoo** [3]

[1]Department of Mathematics, Kanchrapara College, Kanchrapara, North 24, Parganas, West Bengal, India

[2]Department of Mathematics, C. V. Raman Global University, Bidyanagar, Mahura, Janla, Bhubaneswar, 752054, Odisha, India

[3]School of Basic Sciences & Humanities, Odisha University of Technology and Research, Techno Campus, Ghatikia, Bhubaneswar, 751029, Odisha, India

[*]Corresponding author E-mail: mahantakamal@gmail.com

Received: 31 July 2024

doi: https://doi.org/10.55318/bgjp.2024.51.3.296

Abstract. The Bardeen-AdS black hole is a sort of generalization of the basic Bardeen black hole where the cosmological constant is present, making the black hole reside in an anti-de Sitter (AdS) spacetime. Cosmological constants and quintessence are the two main contenders for dark energy. Here, we explored the behavior of the time-like and null geodesics of Bardeen-Ads's black hole with quintessence. We have created 'effective potential' diagrams when laid out with different parameters, which showed the possibilities of having bound orbit for both circular and radial geodesics. In this work, we considered the impact of magnetic monopole charge and normalization constant (quintessence) on the geodesic study of the black hole and further checked the super-radiant effect.

KEY WORDS: Bardeen black hole, Quintessence, Null geodesic, Time-like geodesic, Effective potential.

1 Introduction

The astrophysics has preferred the black hole as one of the most strong discoveries. A black hole is such a region of spacetime wherein it possesses an extremely large gravitational field so powerful that nothing, including light, can ever get out from it. In general, the black hole is a collection of spacetime singularities and event horizons. The event horizon is out surface with infinite red shift and this leads to getting all physical information. Black holes may be characterized in

terms of three classical attributes that include mass, charge, and angular momentum [1,2]. The present-day cosmological analysis of supernovae type Ia(SNe Ia), the cosmic microwave background (CMB), and Hubble data indicates that the present universe is in a phase of going for accelerating expansion implying the existence of some form of energy with large negative pressure referred in literature as dark energy. In order to find out what kind of energy is hidden behind this and to assess the effect of it on the other measurable quantities has turned into one of the most appealing questions at present among the researchers focused mostly on cosmology and particle physics. The list of dark energy candidates is rather large and it includes cosmological constant. Quintessence is one of the important candidates for dark energy [3–7].

In the past few years few models associated with the presence of dark energy and what is known as Quintessence are put forward. It has therefore been interesting to consider the motion of test particles in the presence of Bardeen AdS black hole surrounded by quintessence, and this has been explained in this paper. However, its impact is far much less pronounced in our local universe, but the fact remains that dark energy does in some way influence the dynamics of our universe at some degree [3,8–13]. As in GR, the matter field makes space-time to be curved thus the curvature and geometry of the space-time are important. This force which in return is represented by the curvature in a given 'space-time' is the Geodesic Equations that explain the relative acceleration of two neighboring geodesics in different situations [14–22].

In curved spacetime, a geodesic is the path followed by free-moving particles which only experience gravity. The analysis of time-like and null geodesics is a good start for the investigation of the geometric properties of black hole spacetime which possesses the main geometric features of geometrically thin (thick) accretion disk [23].

In this work, we focus on the static spherically symmetry solution as Xie et al. used in their work [24], which corresponds to the Bardeen-AdS black hole encircled by the quintessence given by

$$ds^2 = -g(r)dt^2 + \frac{1}{g(r)}dr^2 + r^2(d\theta^2 + \sin^2\theta d\phi^2)$$

with

$$g(r) = 1 - \frac{2Mr^2}{(r^2+a^2)^{3/2}} + \frac{r^2}{l^2} - \frac{b}{r^{3\omega_q+1}},$$

ω_q is the quintessence state parameter that takes values in the range $-1 < \omega_q < -1/3$, a is positive magnetic monopole charge, b is positive normalization constant connected to the quintessence. In this work, we investigate the model for the particular value of $\omega_q = -2/3$.

For $\omega_q = -2/3$, we have

$$ds^2 = -g(r)dt^2 + \frac{1}{g(r)}dr^2 + r^2(d\theta^2 + sin^2\theta d\phi^2), \tag{1}$$

with

$$g(r) = 1 - \frac{2Mr^2}{(r^2+a^2)^{3/2}} + \frac{r^2}{l^2} - br\,,$$

where M refers mass of black hole, l is AdS radius defined by the relation $\Lambda = -3/l^2$. Here, we have looked at the time-like and null geodesics of Bardeen-Ads's black hole with quintessence. We have drawn 'effective potential' diagrams, which when plotted with different parameters displayed the possibilities to have bound orbit for both circular as well as radial geodesics. In this work we intend to study the effect of the magnetic charge of the monopole and normalization constant or quintessence on the geodesic study of black holes, and also examine the super-radiant effect.

2 Geodesic Motion

Now, the geodesic equations for the metric (1) is given by

$$\frac{d^2x^\alpha}{d\delta^2} + \Gamma^\alpha_{\mu\nu}\frac{dx^\mu}{d\delta}\frac{dx^\nu}{d\delta} = 0\,. \tag{2}$$

In the plane $\theta = \pi/2$, the geodesic trajectories typically satisfy the following equations derived from the metric of the black hole (1):

$$\begin{aligned} r^2\frac{d\phi}{d\delta} &= J\,,\\ \frac{dt}{d\delta} &= \frac{e}{g(r)}\,,\\ \left(\frac{dr}{d\delta}\right)^2 &= e^2 - \left(\frac{J^2}{r^2} + L\right)g(r)\,. \end{aligned} \tag{3}$$

Given that e and J represent the energy per unit mass and angular momentum of the particle, respectively, and considering the Lagrangian L is taken as 0 for mass less particles (like photons) and 1 for massive particles. Taking $J = 0$ in equations (3) for radial geodesic, we have

$$\left(\frac{dr}{d\delta}\right)^2 = e^2 - Lg(r)\,. \tag{4}$$

In the case of radial geodesic, we may also write

$$\dot{r}^2 \equiv \left(\frac{dr}{d\delta}\right)^2 = e^2 - Lg(r) \tag{5}$$

and

$$\left(\frac{dr}{dt}\right)^2 = \left(1 - \frac{2Mr^2}{(r^2+a^2)^{3/2}} + \frac{r^2}{l^2} - br\right)^2 \times \left[1 - \frac{L}{e^2}\left(1 - \frac{2Mr^2}{(r^2+a^2)^{3/2}} + \frac{r^2}{l^2} - br\right)\right]. \quad (6)$$

2.1 Motion of photon-like test particle ($L = 0$)

Putting $L = 0$ in equation (5) for photon like test particle, we get

$$\dot{r}^2 \equiv \left(\frac{dr}{d\delta}\right)^2 = E^2\,. \quad (7)$$

From equation (7), we obtain the following relationship:

$$\pm E\delta = r\,.$$

We present the variability of radial distance (r) with respect to the proper time (δ) in Figure 1a taking $e = 2$.

Again for photon particle, equation (6) gives

$$\left(\frac{dr}{dt}\right)^2 = \left(1 - \frac{2Mr^2}{(r^2+a^2)^{3/2}} + \frac{r^2}{l^2} - br\right)^2,$$

which gives

$$\pm t = \int \frac{dr}{\left(1 - \frac{2Mr^2}{(r^2+a^2)^{3/2}} + \frac{r^2}{l^2} - br\right)}\,. \quad (8)$$

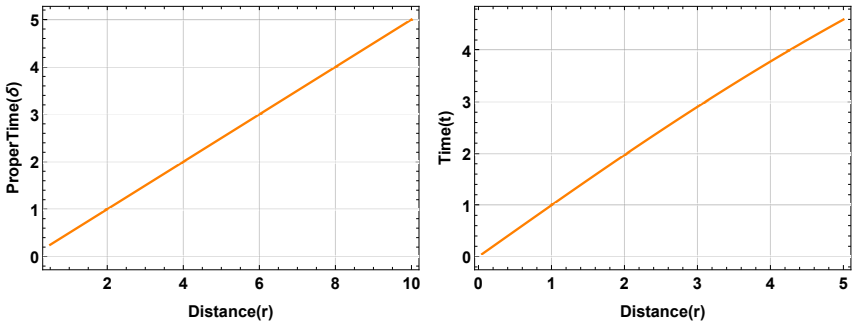

(a) (b)

Figure 1. Variation of ordinary time and proper time w.r.t radial distance.

Since the nature of the integrand of the integration (8) is non-linear, it is very tough to integrate it. We assume

$$\frac{r^2}{l^2} - br \equiv 2Mr^2 \left(\frac{1}{\left(r^2+a^2\right)^{3/2}} + \frac{b^2}{2a^2l^2} \right)$$

for the certain neighborhood of $1/r$ so that effect of magnetic mono-pole charge and normalization constant (quintessence) may reserved, and then integrating (8), we obtain

$$\pm\, t = \frac{al}{bM^{1/2}} \tan^{-1}\left(\frac{rb\sqrt{M}}{al} \right) . \tag{9}$$

Again, we present the variability of radial distance with respect to the time of this particle in Figure 1b taking $l = 10, M = 0.5, a = 0.2, b = 0.3$.

In the context of geodesic motion, especially for a photon-like particle, Figure 1 represents how the ordinary time (t) and the proper time (δ) increase monotonically as the object moves away or comes closer to the black hole along the radial coordinate (r).

2.2 Motion of massive test particle ($L = 1$)

Putting $L = 1$ in equation (5), we get

$$\dot{r}^2 \equiv \left(\frac{dr}{d\delta}\right)^2 = e^2 - \left(1 - \frac{2Mr^2}{\left(r^2+a^2\right)^{3/2}} + \frac{r^2}{l^2} - rb \right) . \tag{10}$$

Considering

$$\frac{r^2}{l^2} - rb \equiv 2Mr^2 \left(\frac{1}{\left(r^2+a^2\right)^{3/2}} + \frac{1}{2a^2l^2} \right)$$

for a certain neighbourhood of $1/r$, and then integrating (10), we get

$$\pm\delta = \frac{la}{b\sqrt{M}} . \sin^{-1}\left(\frac{rb\sqrt{M}}{la\sqrt{e^2-1}} \right) \tag{11}$$

From equation (11), we get the proper time (δ)-distance (r) relationship which has been plotted in Figure 2a with $l = 10, M = 1, a = 0.2, b = 0.3, e = 2$.

Now, putting L=1 in equation (6), we get

$$\left(\frac{dr}{dt}\right)^2 = \left(1 - \frac{2Mr^2}{\left(r^2+a^2\right)^{3/2}} + \frac{r^2}{l^2} - br \right)^2 \times \left[1 - \frac{1}{e^2} \left(1 - \frac{2Mr^2}{\left(r^2+a^2\right)^{3/2}} + \frac{r^2}{l^2} - br \right) \right] . \tag{12}$$

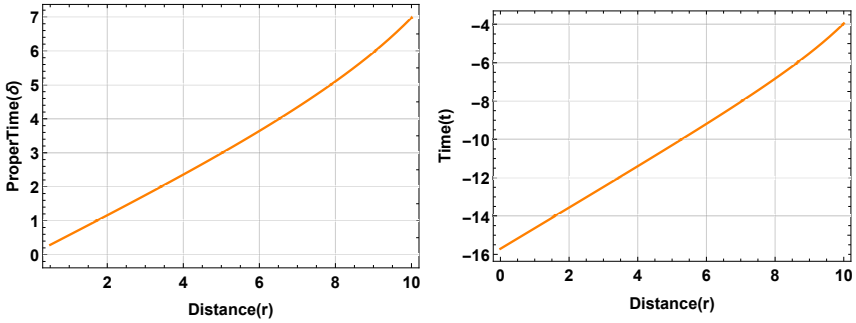

(a) (b)

Figure 2. Variation of ordinary time and proper time w.r.t radial distance.

Taking

$$\frac{r^2}{l^2} - br \equiv 2Mr^2\left(\frac{1}{(r^2+a^2)^{3/2}} + \frac{1}{2a^2l^2}\right)$$

for a certain neighbourhood of $1/r$, and then, we get

$$\left(\frac{dr}{dt}\right)^2 = \left(1+\frac{Mb^2r^2}{a^2l^2}\right)^2\left(1-\frac{1}{e^2}\left(1+\frac{Mb^2r^2}{a^2l^2}\right)\right),$$

which gives

$$\pm\, t \;= \int \frac{dr}{\left(1+\frac{Mb^2r^2}{a^2l^2}\right)\sqrt{1-\frac{1}{e^2}\left(1+\frac{Mb^2r^2}{a^2l^2}\right)}}\,.$$

Taking $r = 1/y$, we get

$$\pm\, t \;= -ea^3l^3\int \frac{ydy}{\left(l^2a^2y^2+Mb^2\right)\sqrt{e^2a^2l^2y^2 - l^2a^2y^2 - Mb^2}}\,.$$

Taking, $v^2 = \left(e^2-1\right)l^2a^2y^2 - Mb^2$, we get

$$\pm t \;= -eal\int \frac{dv}{v^2+e^2Mb^2} = -\frac{la}{b\sqrt{M}}\tan^{-1}\left(\frac{v}{eb\sqrt{M}}\right)$$

or

$$\pm t \;= -\frac{la}{b\sqrt{M}}\tan^{-1}\left(\frac{\sqrt{\left(e^2-1\right)l^2a^2y^2 - Mb^2}}{eb\sqrt{M}}\right), \tag{13}$$

i.e.,

$$\pm t \;= -\frac{la}{b\sqrt{M}}\tan^{-1}\left(\frac{\sqrt{\left(e^2-1\right)l^2a^2 - Mb^2r^2}}{ebr\sqrt{M}}\right). \tag{14}$$

Equation (14) gives the time (t) – distance (r) relationship which has also been plotted in Figure 2b with $l = 10, M = 1, a = 0.02, b = 0.02, e = 1.5$. From the specific calculations made on the geodesic motion, especially for the massive particles, it is seen from Figure 2 that the ordinary time (t) and the clock proper time (δ) increase monotonically with the radial distance (r) from the black hole as the particle approaching or away from the black hole. This is seen in Figure 2b that when t goes to zero from the negative domain an observer or particle drops into the black hole from the particular zone where the time coordinates act differently at a large distance from the black hole.

3 Construction of Effective Potential and Its Behaviors

In this section, we build up the effective potential for analyzing the behavior of our model relying on the rationale given by Kalam et al. [25, 26]. The effective potential V_{eff} be taken as

$$V_{\text{eff}} = -\frac{1}{2}\left(\frac{dr}{d\delta}\right)^2 = -\frac{1}{2}\left[e^2 - \left(Lg(r) + \frac{J^2}{r^2}g(r)\right)\right], \tag{15}$$

where

$$g(r) = 1 - \frac{2Mr^2}{(r^2+a^2)^{3/2}} + \frac{r^2}{l^2} - rb\,.$$

3.1 V_{eff} for photon like test particle ($L = 0$)

3.1.1 Case-(i) $L = J = 0$

In this case, we take $J = 0$ for radial geodesics, and then,

$$V_{\text{eff}} = -\frac{1}{2}e^2\,,$$

we find that the effective potential is zero when energy e is zero and hence it means at this energy the geodesic motion implies that the particle or the test body is not affected by the gravitational potential. In this case, the geodesics are solely linked with spacetime structure and not the gravitational force exerted by the mass or charge of the black hole.

3.1.2 Case-(ii) $L = 0$, $J \neq 0$

For circular motion, we take $J \neq 0$, and then we get

$$V_{\text{eff}} = -\frac{1}{2}e^2 + \left(1 - \frac{2Mr^2}{(r^2+a^2)^{3/2}} + \frac{r^2}{l^2} - rb\right)\frac{J^2}{2r^2}\,. \tag{16}$$

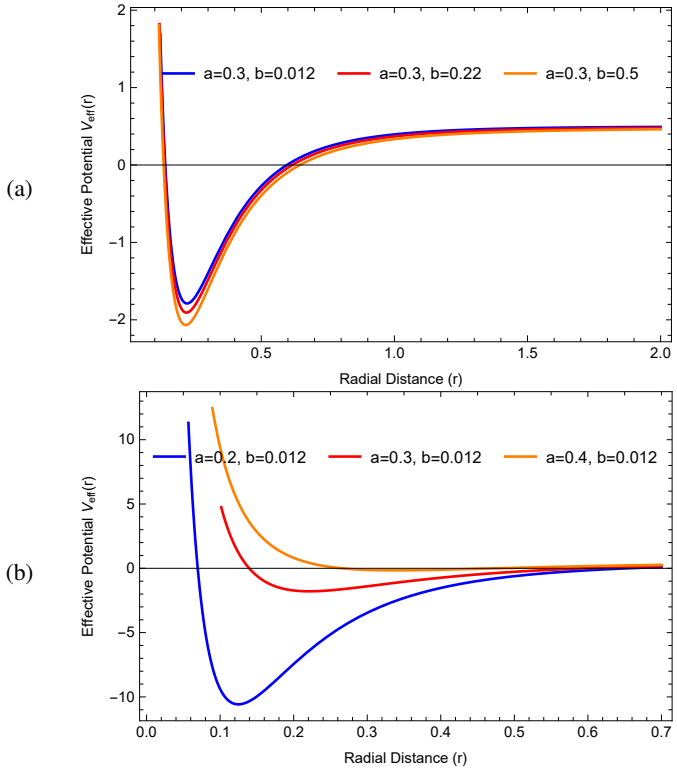

Figure 3. Effective potential taking $e = 0.13$, $M = 1$, $l = 0.5$, $J = 0.5$.

Now, using the equation (16), We plot the effective potential function in Figure 3, where the points of intersection of the effective potential curve with radial-axis give the position of horizons and found that V_{eff} is negative between two horizons and have minima there. Thus, they have a stable circular orbit. Continuing the discussion of Figure 3a, it is clear that if the strength of the quintessence normalization constant ('b') increases, then the value of effective potential decreases. However, from Figure 3b, it is clear that when the value of magnetic monopole charge ('a') is increased, the value of the effective potential decreases. Moreover, it is possible to find here that the number of event horizons decreases with the increased value of magnetic monopole charge.

3.2 V_{eff} for massive test particle ($L = 1$)

In this case, for radial geodesics, we take J=0, and then, the effective potential is given by

$$V_{\text{eff}} = -\frac{1}{2}\left(e^2 - \left(1 - \frac{2Mr^2}{(r^2+a^2)^{3/2}} + \frac{r^2}{l^2} - rb\right)\right).$$

3.2.1 Case-(i) when $e = 0$

In first case, if we take $e = 0$ then V_{eff} becomes

$$V_{\text{eff}} = \frac{1}{2}\left(1 - \frac{2Mr^2}{(r^2+a^2)^{3/2}} + \frac{r^2}{l^2} - rb\right). \tag{17}$$

Now, using the equation (17), we plot the effective potential function in Figure 4. As for the radial geodesics, angular momentum is zero, and effective potential will be zero for some finite value of r in the range $0 \leq r < r_-$ as $g(r) > 0$. As in the previous case, we find a similar effect of strength of quintessence normalization constant ('b') and magnetic monopole charge ('a') on the black hole horizons and thus there is the possibility of having the circular orbit.

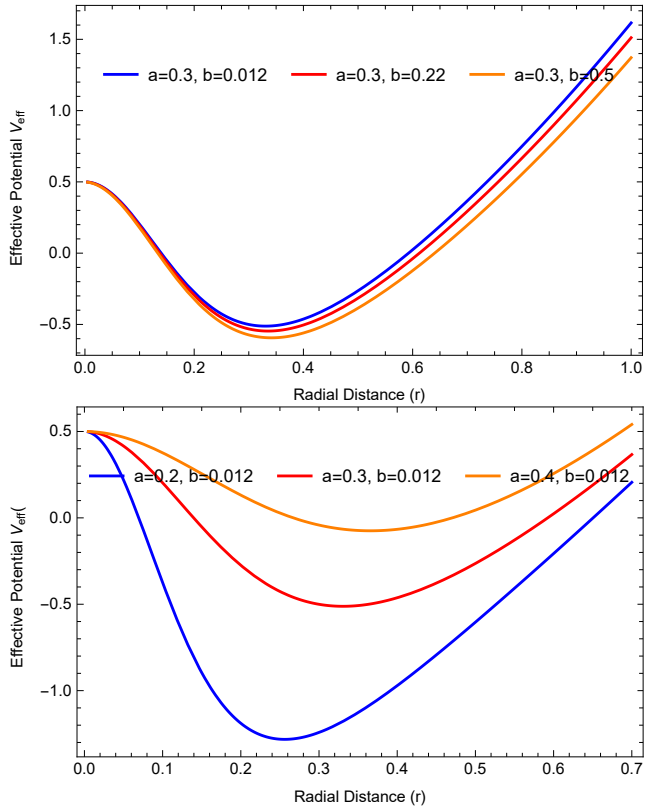

Figure 4. Effective potential taking $M = 1, l = 0.5$.

3.2.2 Case-(ii) when $e \neq 0$

In this case, V_{eff} is

$$V_{\text{eff}} = \frac{1}{2}\left(-e^2 + 1 - \frac{2Mr^2}{(r^2+a^2)^{3/2}} + \frac{r^2}{l^2} - rb\right).$$

In this case, $e \neq 0$ and the general form of the effective potential function is presented in Figure 5. In a similar manner as in the previous cases, the strength of the quintessence normalization constant ('b') and the magnetic monopole charge ('a') have effects on the black hole horizons and hence there is the possible existence of the circular orbit.

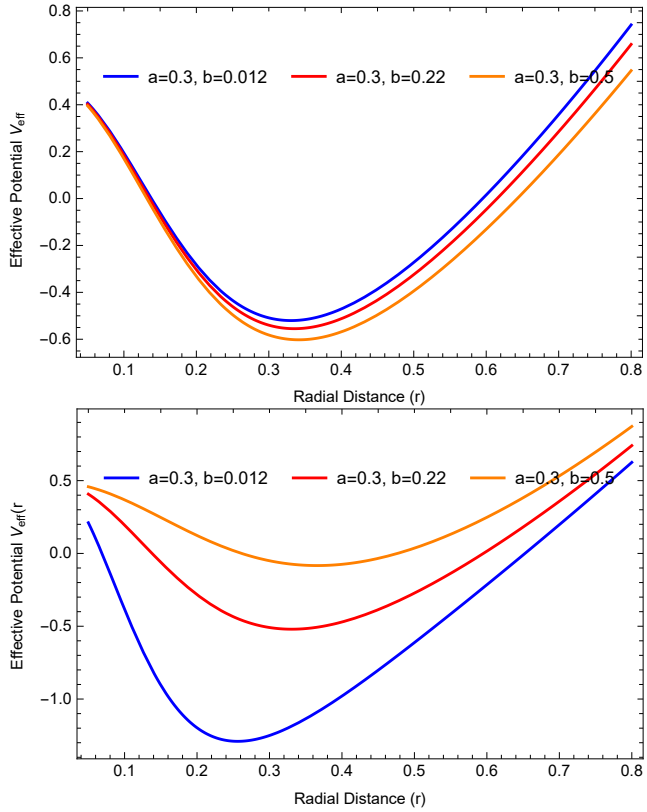

Figure 5. Effective potential taking $e = 0.13$, $M = 1$, $l = 0.5$.

4 Checking of Existence of Superradiance

In 1971, Zel'dovich found out that if radiation bounces off absorbing rotating surfaces, waves with larger amplitude may appear under particular circumstances [27]. This phenomenon is now commonly known as superradiance and entails incident radiation. It is supposed that monochromatic of frequency ω must obey $\omega < m\Omega$, where m is the azimuthal number concerning the rotation axis and Ω is the angular velocity of the body. It has been found that the superradiance of the black hole is related to newly discovered asymptotically flat, hairy black holes [28]. Superradiance connects phase transitions between spinning or charged black objects in asymptotically anti-de Sitter (AdS) spacetime [29, 30]. In addition, in Superradiance, the authors relate the black-hole area theorem, the Penrose process, tidal forces and Hawking radiation. There are various ways in which the amplified radiation can be confined, for instance by magnetic fields or via anti-de Sitter boundaries and this leads to strong instabilities. One notes that stringy Reissner-Nordström black hole is superradiantly unstable under charged massive scalar perturbation for introducing a mirror [31,32]. In the present case, following the previous works [25, 26], we are interested in checking the existence of super-radiance.

The massless scalar wave equation for the model (1) is

$$g^{-1/2}\frac{\partial}{\partial x^k}\left(g^{1/2}g^{kj}\frac{\partial}{\partial x^j}\right)\pi = 0\,, \tag{18}$$

where g_{kj} stands as usual meanings. The equation (18) can also be expressed as

$$-\frac{r^4\sin\theta}{A}\frac{\partial^2\pi}{\partial t^2} + \sin\theta\frac{\partial}{\partial r}\left(A\frac{\partial\pi}{\partial r}\right) + \frac{\partial}{\partial\theta}\left(\sin\theta\frac{\partial}{\partial\theta}\right)\pi + \frac{1}{\sin\theta}\frac{\partial^2\pi}{\partial\phi^2} = 0\,,$$

where $A = r^2 - \dfrac{2Mr^4}{(r^2+a^2)^{3/2}} + \dfrac{r^4}{l^2} - br^3$.

Now, as per the previous works [25, 26], we have taken

$$\chi = e^{-i\omega t}e^{im\phi}R(r)\Theta(\theta)$$

and obtained the radial equation using the method of separation of variables

$$A\frac{\partial}{\partial r}\left(A\frac{\partial R}{\partial r}\right) + (r^4\omega^2 - A\lambda)R = 0$$

and the angular part becomes

$$\frac{1}{\sin\theta}\frac{\partial}{\partial\theta}\left(\sin\theta\frac{\partial\Theta}{\partial\theta}\right) - \frac{m^2}{\sin^2\theta}\Theta + \lambda\Theta = 0\,.$$

Therefore, the radial equation is

$$A\frac{d}{dr}\left(A\frac{dR}{dr}\right)+\left(\omega^2 r^4-\lambda A\right)R=0 \tag{19}$$

Now, Tortoise coordinate (r^*) is defined as

$$\frac{dr^*}{dr}=\frac{r^2}{A}\,,\quad \text{i.e.,}\quad A\frac{d}{dr}=r^2\frac{d}{dr^*}\,,$$

where variable r^* is non-integrable. If we consider a function $u(r)=rR$, then the radial equation (19) reduced to

$$\frac{d^2u}{dr^{*2}}+\left[\frac{2A^2}{r^6}-\frac{A}{r^5}\frac{dA}{dr}-\frac{A\lambda}{r^4}+\omega^2\right]u=0\,. \tag{20}$$

Now,

$$\frac{dA}{dr}=r+\frac{A}{r}-\frac{5r^3}{l^2}-2br^2\,. \tag{21}$$

From equations (20) and (21), we have

$$\frac{d^2u}{dr^{*2}}+\left[\frac{A^2}{r^6}-\frac{A}{r^4}\left(1+\lambda\right)+\frac{2Ab}{r^3}+\frac{5A}{r^2l^2}+\omega^2\right]u=0\,. \tag{22}$$

Here

$$U(r)=-\left[\frac{A^2}{r^6}-\frac{A}{r^4}\left(1+\lambda\right)+\frac{2Ab}{r^3}+\frac{5A}{r^2l^2}+\omega^2\right]$$

represents a potential barrier. At the horizon ($A\to 0$, $r^*\to-\infty$), the radial equation (22) is

$$\frac{d^2u_h}{dr*2}+\omega^2u_h=0$$

with $U(r)=-\omega^2$ and u_h represents the radial solution at the horizon.

Now, asymptotically, $r\to\infty$, implies that $r^*\to\infty$. In this case, $U(r)\neq-\omega^2$. Thus, we did not get a similar form as found in the previous case and u_∞ is not the solution to the equation (22) at ∞. Hence $u_h\neq u_\infty$ implies that there is super-radiance for an incident massless scalar field, and hence charge extraction from black holes is possible through amplification of scalar waves.

5 Conclusion

In this investigation, we have analyzed the time-like and null geodesics around a charged Bardeen-AdS black hole immersed in quintessence. As it can be seen from Figure 1, the coordinate time t and the proper time δ are increasing as

the photon is moving radially in the spacetime of Bardeen-AdS black hole surrounded by quintessence, which means that the spacetime is consistent and regular. It suggests that light interacts causally and continuously with spacetime, that effects normally related to gravity such as redshift and time dilation, and that the spacetime is not singular or otherwise pathological in the region under discussion. From Figure 2, one can see as in the previous case that the ordinary time t and the clock proper time δ increase monotonically with respect to the radial distance r. This is seen in Figure 2b which shows that when t goes to zero from the negative domain it may well mean that an observer or particle drops into the black hole from the particular zone where the time coordinates acts differently at a large distance from the black hole. For radial geodesic and photon-like particles, the effective potential vanishes if the energy $e = 0$, and then, these geodesics are found to be independent of the mass and charge of the black hole. Hence, it means that in this particular energy state(e=0), the geodesic motion witnesses the fact that the particle or test body is not affected by the gravitational potential. In this case, the geodesics are solely linked with spacetime structure and not the gravitational force exerted by the mass or charge of the black hole. Specifically for non-radial and photon-like particles, potential V_{eff} is negative in between two horizons and exhibits a minimum there. Therefore, they have stable circular orbits. Going on with the discussion of Figure 3a, it can be understood that if the strength of the quintessence normalization constant ('b') increases then the value of the effective potential decreases. But as deduced from Figure 3b, we see that the increase in the value of the magnetic monopole charge ('a'), results in the decrease in the value of the effective potential. Hence one can conclude here that the number of the event horizons diminishes as the value of the magnetic monopole charge increases. For radial geodesic, we also study the effective functions for both $e = 0$ and $e \neq 0$ and figures drawn in Figure 4 and Figure 5 respectively to find similar behavior of effect of the magnetic monopole charge and strength of quintessence normalization constant. Finally, we have also confirmed whether there is any Superradiance, which is an interaction where the waves are made to gain energy or charge from the charged Bardeen AdS black hole placed inside the quintessence black hole. We have identified that there exists phenomena of super-radiance and even scalar waves may also be involved in energy extraction.

References

[1] R.A. Capobianco (2019) Geodesic motion in the Reissner-Nordström space-time. Ph.D. thesis, Universidade de São Paulo.

[2] J.B. Griffiths, J. Podolskỳ (2009) *Exact space-times in Einstein's general relativity*. Cambridge University Press.

[3] R. Uniyal, N. Chandrachani Devi, H. Nandan, K. Purohit (2015) Geodesic motion in Schwarzschild spacetime surrounded by quintessence. *Gen. Relativ. Gravit.* **47** 1-20.

[4] T. Padmanabhan (2003) Cosmological constant—the weight of the vacuum. *Phys. Rep.* **380** 235-320.

[5] J. Cunha, J. Alcaniz, J.A.S. Lima (2004) Cosmological constraints on Chaplygin gas dark energy from galaxy cluster x-ray and supernova data. *Phys. Rev. D* **69** 083501.

[6] S. Capozziello, V.F. Cardone, E. Piedipalumbo, C. Rubano (2006) Dark energy exponential potential models as curvature quintessence. *Class. Quantum Grav.* **23** 1205.

[7] A. Vikman (2005) Can dark energy evolve to the phantom? *Phys. Rev. D* **71** 023515.

[8] A. De Felice, S. Tsujikawa (2010) f(R) theories. *Living Rev. Relat.* **13** 1-161.

[9] S. Nojiri, S.D. Odintsov (2007) Modified gravity as an alternative for ΛCDM cosmology. *J. Phys. A* **40** 6725.

[10] R. Durrer, R. Maartens (2008) Dark energy and dark gravity: theory overview. *Gen. Relativ. Gravit.* **40** 301-328.

[11] S. Nojiri, S.D. Odintsov (2007) Introduction to modified gravity and gravitational alternative for dark energy. *Int. J. Geom. Methods Mod. Phys.* **4** 115-145.

[12] S. Capozziello, S. Carloni, A. Troisi (2003) Quintessence without scalar fields. *arXiv preprint astro-ph/0303041* .

[13] M. Sami (2007) Models of dark energy. In: *The Invisible Universe: Dark Matter and Dark Energy*, ed. L. Papantonopoulos, Springer, pp. 219-256.

[14] K.S. Thorne (1988) Gravitomagnetism, jets in quasars, and the Stanford Gyroscope Experiment. In: *Near zero: new frontiers of physics*, eds. J.D. Fairbank, B.S. Deaver, C.W.F. Everitt, P.F. Michelson, W.H. Freeman and Company, New York, pp. 573-586.

[15] J.B. Hartle (2021) *Gravity: an introduction to Einstein's general relativity*. Cambridge University Press.

[16] E. Poisson (2004) *A relativist's toolkit: the mathematics of black-hole mechanics*. Cambridge University Press.

[17] R.M. Wald (1999) Gravitation, thermodynamics and quantum theory. *Class. Quantum Grav.* **16** A177.

[18] J.L. Synge (1934) On the deviation of geodesics and null-geodesics, particularly in relation to the properties of spaces of constant curvature and indefinite line-element. *Ann. Math.* **35** 705-713.

[19] H. Bondi, F.A. Pirani, I. Robinson (1959) Gravitational waves in general relativity III. Exact plane waves. *Proc. R. Soc. Lond. A* **251** 519-533.

[20] G.F. Ellis, H. Van Elst (1999) Deviation of geodesics in FLRW spacetime geometries. In: *On Einstein's Path: Essays in Honor of Engelbert Schucking*, ed. by Alex Harvey, Springer, pp. 203-225.

[21] S. Ghosh, S. Kar, H. Nandan (2010) Confinement of test particles in warped spacetimes. *Phys. Rev. D* **82** 024040.

[22] R. Koley, S. Pal, S. Kar (2003) Geodesics and geodesic deviation in a two-dimensional black hole. *Am. J. Phys.* **71** 1037-1042.

[23] R. Wang, F. Gao, J. Liu (2024) Dynamics of geodesics around the Bardeen-AdS black hole immersed in quintessence. *Results Phys.* **58** 107499.

[24] J. Xie, Y. Wang, B. Tang (2023) Chaotic dynamics of strings around the Bardeen-AdS black hole surrounded by quintessence dark energy. *Phys. Dark Universe* **40** 101184.

[25] M. Kalam, N. Farhad, S.M. Hossein (2014) Geodesic study of a charged black hole. *Int. J. Theor. Phys.* **53** 339-349.

[26] M. Kalam, F. Rahaman, A. Ghosh, B. Raychaudhuri (2009) Discussion on Some Characteristics of Charged Brane-World Black Holes. *Int. J. Mod. Phys. A* **24** 719-739.

[27] Ya.B. Zel'dovich (1971) Wave generation by a rotating body. *ZhETF Pis. Red.* **14** 270.

[28] C.A. Herdeiro, E. Radu (2014) Kerr black holes with scalar hair. *Phys. Rev. Lett.* **112** 221101.

[29] V. Cardoso, O.J. Dias (2004) Small Kerr–anti-de Sitter black holes are unstable. *Phys. Rev. D* **70** 084011.

[30] O.J. Dias, P. Figueras, S. Minwalla, P. Mitra, R. Monteiro, J.E. Santos (2012) Hairy black holes and solitons in global AdS5. *J. High Energy Phys.* **2012** 1-87.

[31] R. Li, J. Zhao (2014) Superradiant instability of charged scalar field in stringy black hole mirror system. *Eur. Phys. J. C* **74** 3051.

[32] R. Li, J. Zhao (2015) Numerical study of superradiant instability for charged stringy black hole-mirror system. *Phys. Lett. B* **740** 317-321.